Chemistry Research Journal, 2021, 6(4):31-48

Available online www.chemrj.org

Research Article

ISSN: 2455-8990
CODEN(USA): CRJHA5

Adsorption of Cu (II) ions from aqueous solutions using low cost material

Alaa E. Ali[a,*], Gehan S. Elasala[a], Essam M. Elmeleigy[b], Aml R. Saeed[a]

[a]Chemistry Department, Faculty of Science, Damanhour University
[b]Consultant of Chemical and Environmental Analyzes - Ministry of Healthy

Abstract The adsorption process for copper ions (Cu^{2+}) in the concentration range of 10-200 ppm using bean husk powder as a low-cost adsorbent was studied. The adsorption process was performed under certain conditions of adsorbent dosage, contact time, pH, initial concentration of Cu^{2+}ions and temperature. The FTIR spectra of bean husk showed that the participation of hydroxyl group, carbonyl group and carboxyl group (COOH) in the adsorption process. Thermodynamic parameters (ΔG^o, ΔH^o and ΔS^o) have been calculated indicated the adsorption processes is spontaneous and endothermic process. The adsorption isotherms were best fitted to the Freundlich isotherm. In this study we use adsorption reaction models and adsorption diffusion models to understand the kinetics of the reaction.

Keywords Adsorption removal; Bean husk; Copper; Removal efficiency

Introduction

Contamination of aquatic environment with heavy and toxic metals is a complex problem and their removal requires much attention. Their concentration gets accentuated through bioaccumulation via food chain in living tissues, causing various diseases and physiological disorders [1-3]. Hence the safe and effective disposal of contaminated water containing heavy metals like Lead, Cadmium, Chromium, Mercury is always remained a challenge to the industrialists and environmentalists [4].

The presence of inorganic pollutants such as metal ions in the ecosystem causes a major environmental problem. Toxic metal compounds coming to the earth's surface not only contaminate earth's water (seas, lakes, ponds and reservoirs), but can also contaminate underground water in trace amounts by leaking from the soil after rain and snow [5]. The numerous metals which are significantly toxic to human beings and ecological environments, include chromium (Cr), copper (Cu), lead (Pb),cadmium (Cd), mercury (Hg), zinc (Zn), manganese (Mn) and nickel (Ni), etc [6-7]. Metal ions are released into the environment from many sources. Arsenic is introduced in water through natural and anthropogenic sources release from mineral ores, probably due to long term geochemical changes and from various industrial effluents like metallurgical industries, ceramic industries, dye and pesticides manufacturing industries and wood preservatives [8].

Recently, the adsorption process has gained interest as a more promising method for the long term as its seen to be a more effective and economic approach for heavy metal removal. Adsorption is a fundamental process today due to its flexibility in design and simple operation instead of having to perform adsorptions that are perceived as impractical by most conventional techniques. The term "adsorption" refers as a mass transfer process by which a substance is transferred from the liquid phase to the surface of a solid and becomes bound by physical and/or chemical interactions [9]. The advantages of the adsorption process in removing or minimizing the heavy metals even at low concentration enhance the application of adsorption as one practical treatment. The effectiveness of the adsorption process is mainly influenced by the nature of solution in which the contaminants are dispersed, the

molecular size and the polarity of the contaminant and also the type of adsorbent used. Adsorption also exists due to the attractive interactions between a surface and the species being adsorbed at certain molecular level [10].
The removal of heavy metals by using low cost adsorbent is found to be more encouraging in extended terms as there are several materials existing locally and profusely such as natural materials, agricultural wastes or industrial by-products which can be utilized as low-cost adsorbents [11-12]. To be commercially viable, an adsorbent should have high selectivity to facilitate quick separations, favorable transport and kinetic characteristics, thermal and chemical stability, mechanical strength, resistance to fouling, regeneration capacity and low solubility in the liquid in contact.

Materials and Methods

Biosorbent preparation (Preparation of Bean husk):

The bean husk was selected as adsorbent for removal of Cu^{2+} ions in this study. The bean husk was obtained from a local producer at El Behera Governorate in Egypt, (BH) was collected and washed thoroughly under running tap water to remove dust and any adhering particles then was washed by distilled water. The (BH) was dried under sunlight for a few days and then in oven at 70ºC until it became crisp. The dried (BH) was crushed and blended to fine powder form using a blender. The grinding (BH) in the form of powder was washed with excessive amounts of distilled water; several washings were performed to remove dust and soluble materials and free from any colour and then washed by diluted acid (HCl) for further purity, then washed by distilled water. The powder was dried under sunlight and then in an oven at 70ºC for a period of 1.5 hour and kept in airtight container.

Measures and Analysis

The experiments were done by using:

1. Perkin Elmersege (version 10.5.3) was used to characterize the adsorbent before and after adsorption process.
2. digital magnetic stirrer MS-H-PRO with temperature sensor PT1000.
3. Pinnacle 900T atomic absorption spectrophotometer was used to analyze concentrations of the dissolved Cu^{2+} ions.
4. Crison GLP21 pH meter was used to adjust pH of solutions.

Preparation of synthetic industrial wastewater containing Cu^{+2}ions:

Cu^{2+} ions were used as the adsorbate in this study. 1000 mg/L stock solution of Cu^{2+} ions was prepared by dissolving 3.801 g Cu Nitrate and then diluted to give one liter. Appropriate dilution of the stock solution was carried out by dilution low in order to obtain the desired concentration of Cu^{2+} solution used later in the experiment.

Batch experiments

The adsorption isotherm was determined by shaking a mixture of 0.5g of bean husk and 200 ml of Cu^{2+} solution in constant magnetic stirrer of 400 rpm for 60 min until equilibrium was reached unless otherwise stated. Except for those carried out to examine the effect of the initial concentration of Cu^{2+}. After agitation, the powder was removed by filtration using filter paper. Metal ions concentration in the filtrates as well as in the control samples were determined by using flame atomic absorption spectroscopy (FAAS) spectrometer.
The quantity of metal adsorbed was calculated according to the following equation [13]:

$$\mathbf{q_e = \frac{(C_o - C_e)\,V}{m}} \qquad \textbf{(Eq. 1)}$$

Where:
q_e: sorption capacity (mg/g).
m: weight of adsorbent(g).
C_o: initial concentration (mg/L).

C_e: equilibrium concentration (mg/ L).
v: volume of solution (L).

Results and Discussion

Fourier Transform Infrared (FTIR) Analysis

FTIR analysis was carried out in order to identify the different functional groups present in the selected adsorbent which were responsible for adsorption process [14].

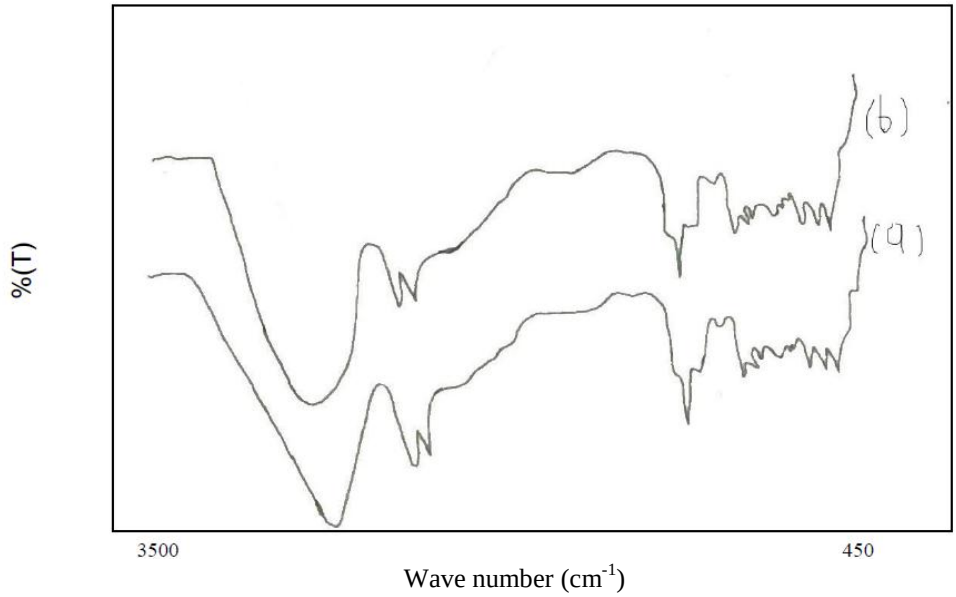

Figure 1: The FTIR spectra of bean husk (a) and after Cu(II) ions uptake (b).

The FTIR spectra of bean husk before metal adsorption showed that, a broad band at 3290 cm^{-1} of (OH) stretch assigned to hydroxyl of polymeric compounds in lignocellulose material [15], (itis composed of carbohydrate polymers (cellulose, hemicellulose), and an aromatic polymer (lignin)) . The 2925, 1711 cm^{-1} Peaks correspond to the stretching vibrations of aliphatic C-H of carboxylic acids, and carbonyl group matching to vibration of ketone, respectively. The (C=O) band at 1464cm^{-1} was assigned to carboxylic group. The band at 1027 cm^{-1} is attributed to C-O stretching vibration in hemicellulose, cellulose and lignin. After metal ion adsorption, the peak at 3290 cm^{-1} on the FTIR spectra of was stretched to 3300 cm^{-1}, indicates the participation of hydroxyl group in the adsorption process. The shift of wave number from 1711 to 1703 $cm^{-1}$for Cu^{2+} indicates the participation of carbonyl group in the adsorption process. Carboxyl group (COOH) was observed at 1464 cm^{-1} before adsorption shifted to 1458, this also suggested that (COOH) may have participated in the adsorption process.

Adsorption Process

The amount of metal adsorbed was obtained from the difference between metal quantity adsorbed by the adsorbent and metal content of the water sample by the equation (1):

$$q_e = [C_o - C_e]v / m \quad \textbf{(Eq. 1)}$$

Where:
C_o: initial concentration (mg/L).
C_e: equilibrium concentration (mg/ L).
v: volume of solution (L).
m: weight of adsorbent(g).
Also the change in % removal with time was determined from the equation (2):

$$\% \text{ Removal} = C_o - C_e / C_o \times 100 \quad \textbf{(Eq. 2)}$$

While amount of heavy metal adsorbed at the surface of the adsorbent at time (t) was determined from the equation (3):

$q_t = [C_o-C_e]/m$ xv (Eq. 3)

Effect of pH

The adsorption process of heavy metal is influenced by the pH of the solution. The adsorption efficiency of Cu^{2+} increased from 51% to 63% as pH increased from 4 to 7. The adsorption capacity of Cu^{2+} onto adsorbent increased significantly with increasing pH value. pH value of the medium affects the equilibrium of the system as the equation (4):

pH = pka - log [AH] /[A^-] (Eq. 4)

Where:

[A^-], [AH], represented the concentration of deprotanted and protanted surface groups and the equilibrium constant pKa.

The effect of solution pH on the adsorption of Cu^{2+}ions onto (BH) was evaluated in the pH range of 4 to 7 and the result was showed in fig (2).

The minimum biosorption at low pH is due to the fact that high concentration and high mobility of H^+ ions, the hydrogen ions are preferentially adsorbed rather than the metal ions. At higher pH values, the lower number of H^+ and greater number of ligands with negative charges results in greater metal ions biosorption [16].

According to the functional groups on the adsorbent surface. Deprotonation of these functional groups occurs on increasing pH and these behave as negatively charged moieties which start attracting the positively charged metal ions [17]. On the other hand, as the pH is lowered, the overall surface charges will become positive, which will inhibit the approach of positively charged metal cations [18]. So, the optimal pH selected was pH 7 for Cu^{2+} ions.

Effect of initial Cu^{2+} ions concentrations

The effect of Cu^{2+} initial concentrations on the adsorption of the metal ions on (BH) powder is showed by fig (3).The variation in the initial metal ions concentration was made from 10 ppm to 200 ppm, while keeping other parameters constant at pH of 7, adsorbent dose of 0.5 g, contact time of 60 minute and agitation speed of 400 rpm.

The removal efficiency of the adsorbent for the Cu^{2+} ions decreased from 50ppm to 200 ppm. At (10, 25) ppm the ratio of the number of moles of solute adsorbed to the surface area of the adsorbent might be large. When concentration increase, the number of moles of solute adsorbed to the surface area of the adsorbent decrease, hence the removal which depend on the initial concentration should obviously decrease with increasing the initial concentration of the heavy metal ions.

The removal efficiency of the ions by the sorbent initially increases with increasing the initial ion concentration. At lower ions concentration in the solution, the ions would interact with the binding sites and thus facilitated almost 100% adsorption, whereas at higher concentrations, more ions are left un-adsorbed in the solution due to the saturation of the binding sites [19].

Effect of speed of agitation

Agitation is an important parameter in adsorption phenomena, influencing the distribution of the solute in the bulk solution and the formation of the external boundary film [20].

The experiments were performed at different rotation speed (100, 200, 300, 400 and 500 rpm)and keeping the other factors constant, pH 7, time 60 min, dose of adsorbent 0.5g, volume 200 ml of 100 ppm of heavy metal, at 25 °C.

It was observed in fig (4) the percentage uptake increased when the rotation speed was increased. During the first 5 minutes, the uptake was 9%, 13%, 15%, 26% and 45%for the agitation rate of 100 rpm, 200 rpm, 300rpm, 400 rpm and 500rpm respectively for the Cu^{2+} ions.

This can be explained by the fact that increasing agitation speed reduces the film boundary layer surrounding particles, thus increases the external film transfer coefficient [21], and the adsorption capacity [22].

Effect of contact time

Equilibrium time is one of the important parameters for selecting a wastewater treatment system [23].

The experiments were performed by varying the contact time from 5 min to 60 min, while keeping other parameters constant at pH of 7, adsorbent dose of 0.5 g, adsorbate concentration (Cu^{2+}) of 100 ppm, volume of solution 200 ml and agitation speed of 400 rpm. The removal efficiency of Cu^{2+}ions has increased rapidly with increasing of shaking time 60 min. After a definite time, the equilibrium might have been reached between the rate of adsorption and rate of desorption, so that the absorption will be difficult.

Maximum adsorption was achieved at 60 minutes' time interval and no significant increase found by further increase in time. Initially, excess of vacant places is available on the surface of sorbent, and uptake of metal ions was more, so there was continuous increase in adsorption capacity by increasing time slot from zero to 60 minutes. But, further increase could not cause sufficient change in adsorption of metals as vacant spaces are already filled, and equilibrium is achieved [24].

Effect of adsorbent dose

The experiments were carried out with different adsorbent dosages (0.1, 0.2, 0.3, 0.5 and 0.7) gm while keeping other parameters constant at pH of 7, initial concentration of 100 ppm, contact time of 60 minutes, volume of solution 2**0**0ml and agitation speed of 400 rpm.

In fig (5) the copper removal increased with increasing the adsorbent dosage reaching maximum removal percentage at dose 0.7 gm of (BH) powder, removal of Cu^{2+} increase from (39% to 86%).

Biomass provides binding sites for the sorption of metal ions, and hence its concentration strongly affects the sorption of metal ions from the solution [25]. For a fixed metal initial concentration, increasing the adsorbent dose provides greater surface area and availability of more active sites, thus leading to the enhancement of metal ion uptake [25].

The decrease in q_e with increase in the adsorbent dose is mainly due to the unsaturation of adsorption sites through the adsorption reaction. Another reason may be due to the particle interactions, such as aggregation, resulting from high sorbent concentration. Such aggregation would lead to a decrease in the total surface area of the adsorbent [26].

Effect of temperature

Temperature plays an important role in controlling the strength of the adsorptive forces between the adsorbent and adsorbate molecules [27-28].

The temperature has an effective effect on the removal efficiency. The experiments were performed at different temperatures of 20 °C, 25°C, 30°C, 35°c and 40°C, while keeping other parameters constant at pH of 7, initial concentration of 100 ppm, contact time of 60 minutes, volume of solution 200ml and agitation speed of 400 rpm. Percentage of removal increased by increasing the temperature as in fig (6).

The highest adsorption of Cu^{2+}ions onto the (BH) surface (Fig 6), occurred in 40 °C. This indicates that the adsorption process is endothermic and favors high temperatures [29].

In fig (6), The removal efficiency increases from 33% to 76% with increasing the temperature. The increase may be due to the rise in the kinetic energy of adsorbent particles and increasing the mobility of the metal cation. Thus, the collision frequency between adsorbent and adsorbate increases; which results in the enhanced adsorption on to the surface of the adsorbent [30-31].

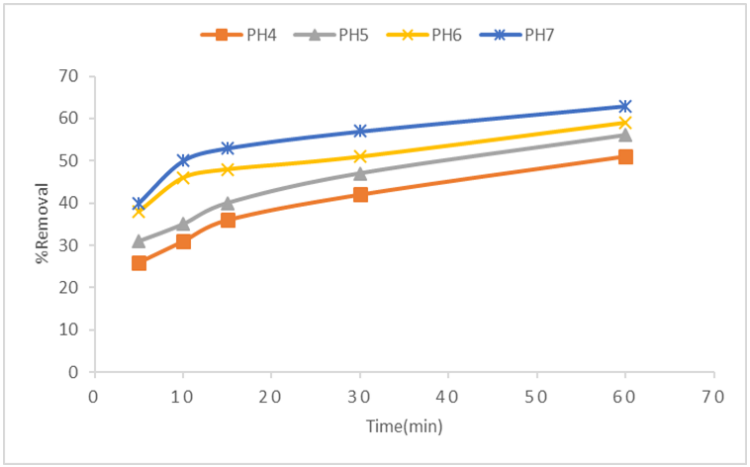

Figure 2: Effect of % removal of Cu(II) against time onto bean husk at different pH (The initial concentration = 100 ppm, dose = 0.5g, stirring speed = 400 rpm, T= 298^{o}K and time = 60 min).

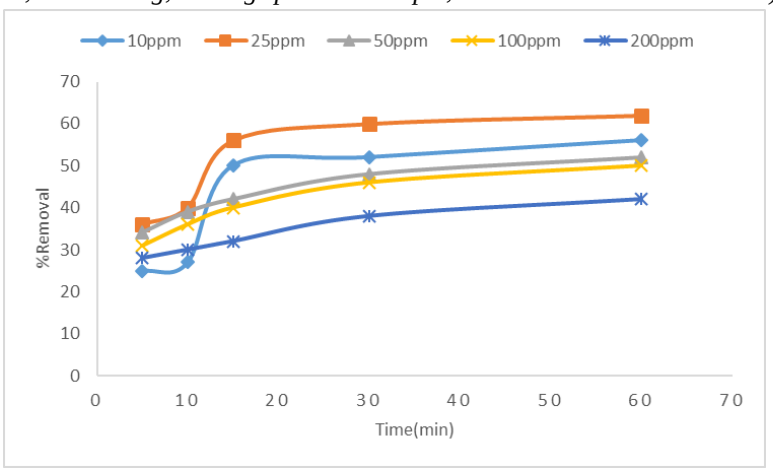

Figure 3: Effect of %removal of Cu(II) against time onto bean husk at different initial concentrations (dose = 0.5g, stirring speed = 400 rpm, T= 298^{o}K and time = 60 min).

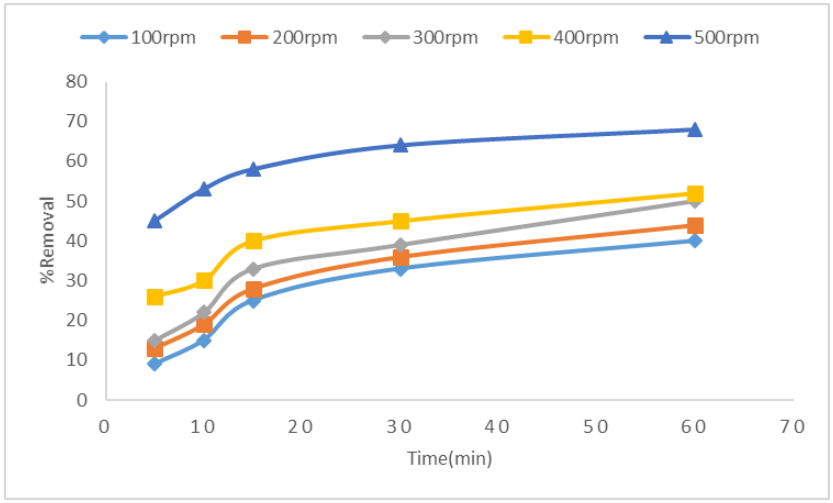

Figure 4: Effect of %removal of Cu(II) against time onto bean husk at different agitation speed (The initial concentration = 100 ppm, dose = 0.5g, T= 298^{o}K and time = 60 min).

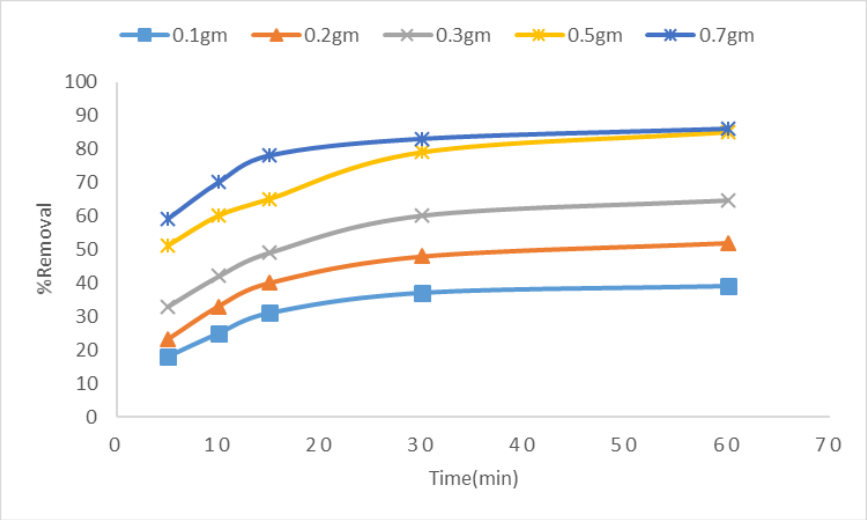

Figure 5: Effect of %removal of Cu(II) against time onto bean husk at different adsorbent dose (The initial concentration = 100 ppm, stirring speed = 400 rpm, T= 298 ^{o}K and time = 60 min).

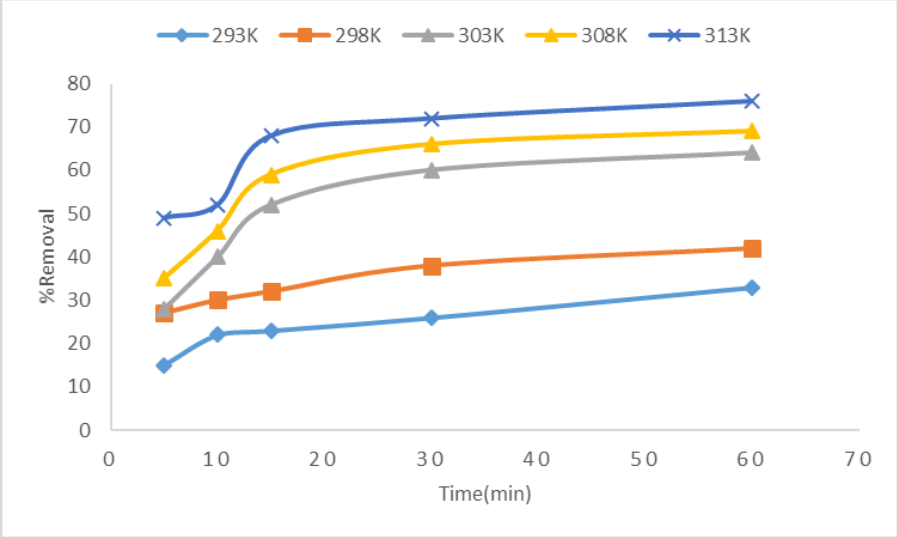

Figure 6: Effect of %removal of Cu(II) against time onto bean husk at different temperatures (The initial concentration = 100 ppm, stirring speed = 400 rpm, dose = 0.5g and time = 60 min)

Thermodynamic Parameters

The thermodynamic parameters such as Gibb's free energy change (ΔG°), enthalpy (ΔH°) and entropy (ΔS°) provide additional information regarding energetic changes involved during the temperature-dependent sorption [32]. These parameters were estimated using the following equations:

$$\mathbf{K_e = \frac{q_e}{C_e}} \qquad \textbf{(Eq. 5)}$$

$$\mathbf{\Delta G^o = -RT \ln K_e} \qquad \textbf{(Eq.6)}$$

$$\mathbf{\Delta G^o = \Delta H^o - T\Delta S^o} \qquad \textbf{(Eq.7)}$$

$$\mathbf{\log K_e = \frac{\Delta S^o}{2.303\ R} - \frac{\Delta H^o}{2.303RT}} \qquad \textbf{(Eq.8)}$$

Where:

q_e (mg/g) is the amount of Cu^{2+}ions adsorbed onto the (BH) powder at equilibrium, C_e (mg/l) the equilibrium concentration of heavy metals ions in the solution, R (J/mol.K) the gas constant 8.314, T (K) the absolute temperature, and K_e (l/g) the adsorption equilibrium constant. ΔH^o and ΔS^o were obtained from the slope and

intercept of the van't Hoff's plot of log (K_e) versus 1/T as shown in fig (7) .The values of ΔG^o, ΔH^o, and ΔS^o were collected in table (1).

The negative value of ΔG° confirm the feasibility of the process and the spontaneous nature of adsorption. The decrease in the negative value of ΔG° with an increase in temperature indicates that the adsorption process of Cu^{2+} ions on (BH) becomes more favorable at higher temperatures [33].

From table (1), the positive value of ΔH° indicates that the adsorption is endothermic process. The positive value of ΔS° suggests that some structural changes occur on the adsorbent, and the randomness at the solid/liquid interface in the adsorption system increases during the adsorption process [34].

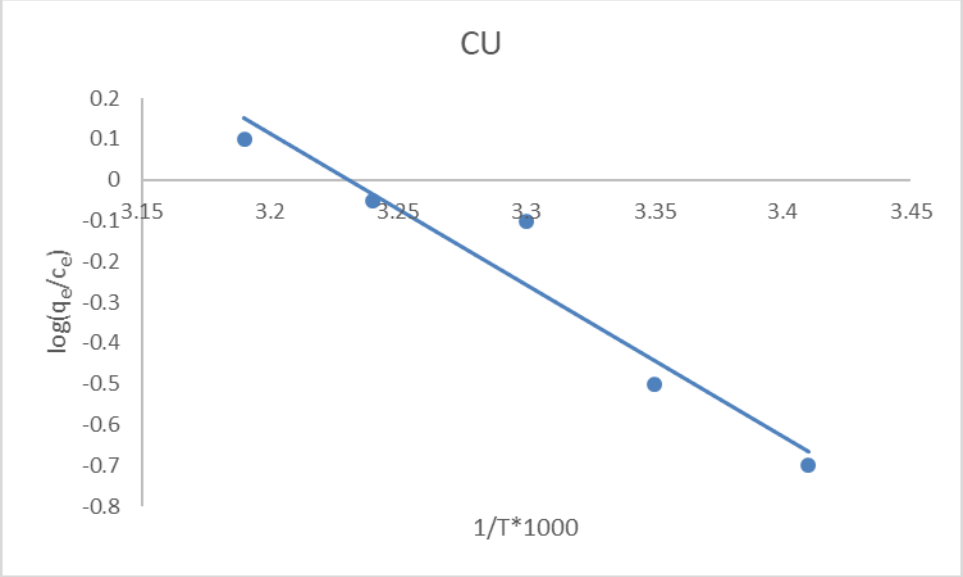

Figure 7: Relationship between log (q_e/c_e) and reciprocal of temperature, at constant initial concentration of 100 ppm, 0.5g of BH and 400 rpm for Cu(II)

Table 1: Thermodynamic parameters of copper onto (BH) powder

Heavy metal	T	Thermodynamic parameters		
	(K)	ΔG^o (kJ/mol)	ΔH^o (kJ/mol)	ΔS^o (kJ/mol. K)
Cu	293	3.799195	71.2	0.229
	298	2.650079		
	303	1.500964		
	308	0.351847		
	313	-0.797267		

Equilibrium Adsorption isothermal

The adsorption isotherm describes how adsorbates interact with an adsorbent and is critical in optimizing the use of adsorbent. Adsorption equilibrium studies are conducted to correlate the adsorption capacity (q_e, $mg \cdot g^{-1}$) and residual adsorbate concentration (C_e, $mg \cdot L^{-1}$) in the liquid phase [35-36].

The sorption equilibrium data collected in this study was fitted into four well-known adsorption isotherms to find the suitable model for this adsorption, namely Langmuir, Freundlich, Temkin and Dubinin-Radushkevich (D-R) isotherm models.

The Langmuir isotherm model assumes a surface with homogeneous binding sites, equivalent sorption energies, and no interaction between sorbate species [18]. In this model once a site is filled, no further sorption can take place at that site. As such, the surface will eventually reach a saturation point where the maximum adsorption of the surface will be achieved [37].

The Langmuir model is obtained under the ideal assumption of a totally homogenous adsorption, which each molecule possess constant enthalpies and sorption activation energy (all sites possess equal affinity for the adsorbate) and represented as following:

$$\frac{C_e}{q_e} = \frac{1}{q_{max}.b} + \frac{C_e}{q_{max}} \quad \textbf{(Eq. 9)}$$

Where:

q_e is the equilibrium metal ion concentration on the adsorbent (mg/g).

C_e is the equilibrium metal ion concentration in the solution.

q_{max} is the monolayer adsorption saturation capacity of the adsorbent .

b is the Langmuir constant.

The essential features of the Langmuir isotherm can be expressed in term of a dimensionless constant separation factor (R_L) which is defined as:

$$R_L = \frac{1}{1+bC_o} \quad \textbf{(Eq. 10)}$$

Where:

R_L is the separation factor, C_o is the initial metal concentration (mg/L) and b is the Langmuir constant (L/mg). $R_L > 1$ indicates an unfavourable monolayer adsorption process, $R_L = 1$ linear, $0 < R_L < 1$ favourable and $R_L = 0$ irreversible [38-39].

Figure (8) by means of linear regression equation. From this regression equation and the linear plot, the values of the Langmuir constants were calculated and were tabulated in table (2). The b and q_{max} were obtained from the slope and intercept of the plots respectively. High R^2value for metal ions reveal the extremely good application of Langmuir model to this adsorption.

The Freundlich isotherm assumes a heterogeneous surface with a non-uniform distribution of heat of biosorption over the surface and a multilayer biosorption can be expressed [40].

The Freundlich isotherm model describes a multi-site adsorption for heterogeneous surfaces and can be represented by equation (11):

$$\log q_e = \log K_f + (1/n) \log C_e \quad \textbf{(Eq.11)}$$

Where:

K_f is the adsorption capacity (L/mg) and 1/n is the intensity of the adsorption showing the heterogeneity of the adsorbent site and the energy of distribution [41].

A plot of $\log q_e$ against $\log C_e$ gave a linear graph with a regression coefficient of 0.9805for copper ions in fig (9).

The n value indicates the degree of nonlinearity between solution concentration and adsorption as follows: if n = 1, then adsorption is linear; if n < 1, then adsorption is a chemical process; if n >1, then adsorption is a physical process [37].

Temkin adsorption isotherm discusses interaction of sorbent and sorbate, and the model is based on assumption that heat of adsorption will not remain constant. It decreases due to interaction between sorbent and sorbate during adsorption phenomenon [42]. The linear form of Temkin model is given by equation (12).

$$q_e = B\ln A_T + B\ln C_e \quad \textbf{(Eq. 12)}$$

Where:

$B=\frac{RT}{bT}$, A_T= Temkin isotherm equilibrium binding constant related to maximum binding energy (L/mg), b_T = Temkin isotherm constant related to heat of sorption (J/mol), T and K are absolute temperature, and(R) the universal gas constant (8.314 $J.mol^{-1}.K^{-1}$), respectively

We obtained A_T, b_T,R^2 from fig (10), A_T= 0.208 L/mg, B= 9.3529, b_T=264.8 J/mol and R^2=0.9214 for (Cu^{2+}) ions, in table (2), which is an indication of the heat of sorption indicating a physical adsorption process and positive value of B indicates an endothermic process [43].

The D.R isotherm model is a semi-empirical equation where adsorption follows a pore filling mechanism. It assumes that the adsorption has a multilayer character, involves van- der Waals forces and is applicable for physical adsorption processes [44-45]. The model is represented by the equation (13) below:

$q_e = q_D exp (- B_D [RT ln (1 + 1/C_e)$ (Eq. 13)

Where, B_D is related to the free energy of sorption per mole of the sorbate as it migrates to the surface of the biomass from infinite distance in the solution and q_D is the Dubinin-Radushkevich isotherm constant related to the degree of sorbate sorption by the sorbent surface [46-47]. The linear form of equation is given as equation (14):

$\ln q_e = \ln q_D - 2B_D RT \ln (1 + 1/C_e)$ (Eq. 14)

A plot of $\ln q_e$ against $RT \ln (1 + 1/C_e)$ for sorbent, yielded straight lines and indicates a good fit of the isotherm to the experimental data. The apparent energy (E_D) of adsorption from Dubinin-Radushkevich isotherm model can be computed using the relation given as equation (15) below [46].

$ED = \sqrt{1/2BD}$ (Eq. 15)

From the linear plot $\ln q_e$ against $RT\ln(1+1/C_e)$ of D-R model in fig (11) and table (2), q_D was determined to be 24.77 mg/g, the mean free energy E_D=0.142 kJ/mol, and the R^2 = 0.9171, for Cu(II) ions. E_D is a parameter used in predicting the type of adsorption. An E_D value < 8 $kJ.mol^{-1}$ is an indication of physisorption [48].

The results indicating that the adsorption also fits to Freundlich model. The constants obtained from the four models are presented in table (2).

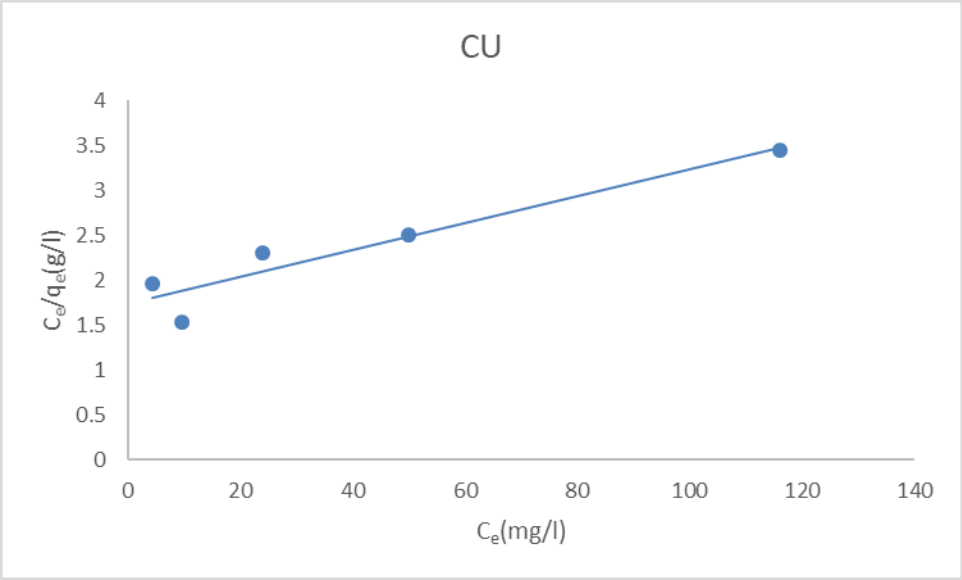

Figure 8: Langmuir adsorption isotherm for Cu^{2+} ions adsorption onto different amounts of (BH) at constant temperature 25°C and contact time 1 h.

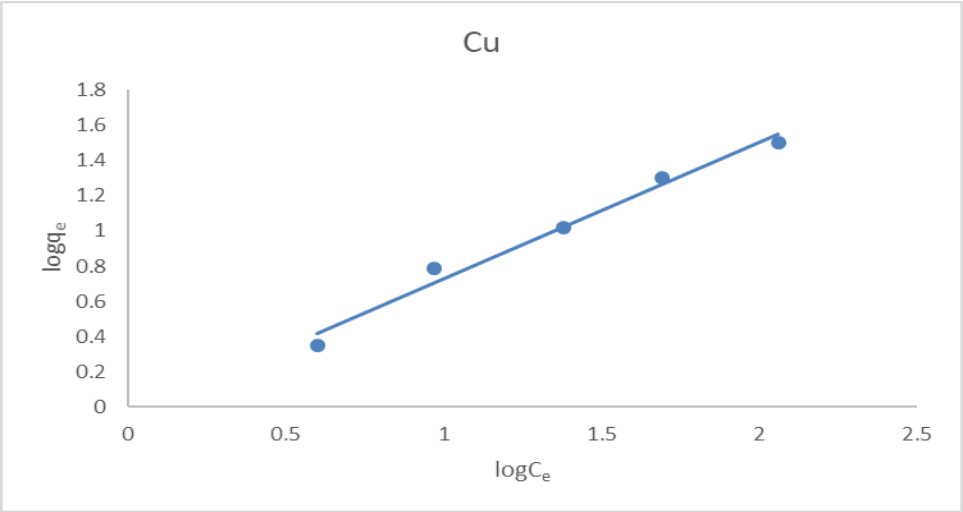

Figure 9: Freundlich adsorption isotherm for Cu^{2+} ions adsorption onto different amounts of (BH) at constant temperature 25 °C and contact time 1h

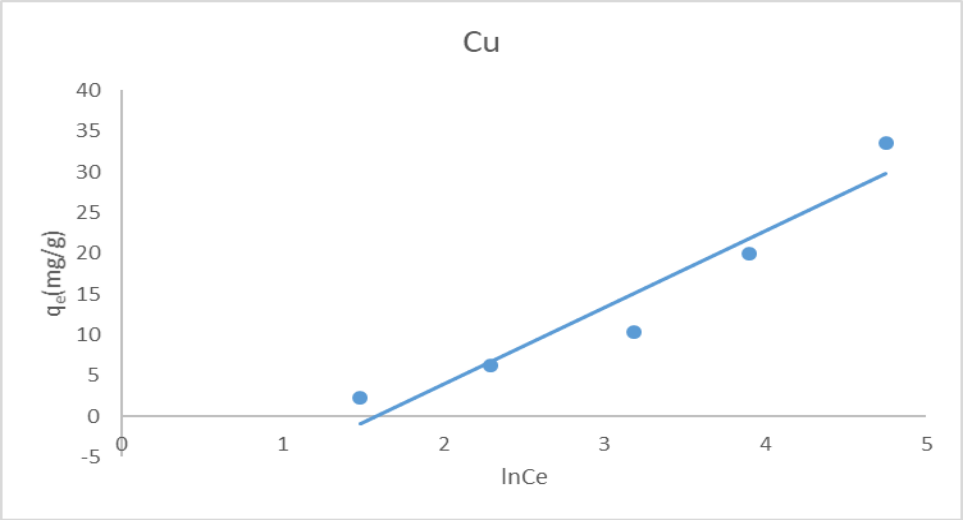

Figure 10: The linearized Temkin adsorption isotherm for Cu(II) by BH at 298^{o}K.

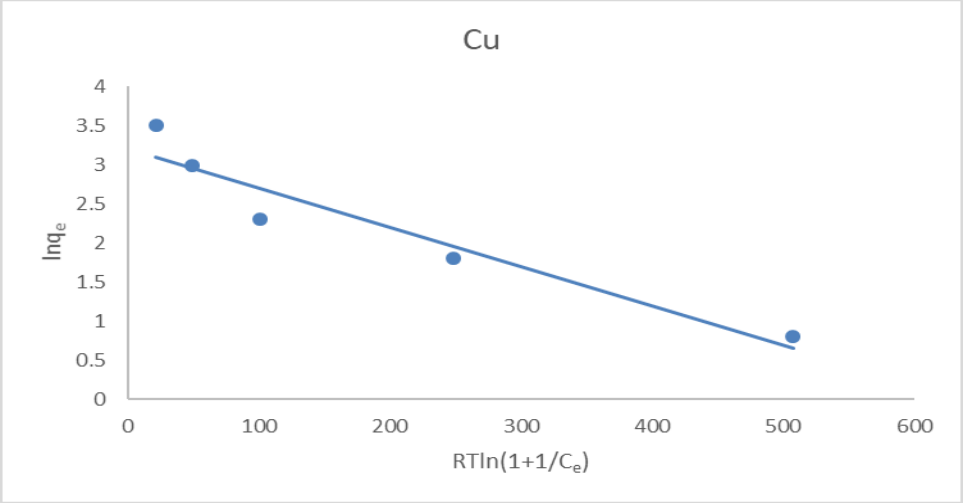

Figure 11: The linear Dubinin-Radushkevich adsorption isotherm for Cu(II) ion with BH at 298^{o}K

Table 2: Adsorption isotherm constants for the adsorption of Cu (II) onto BH at 298^{o}K

Heavy metal	Adsorbent	Langmuir isotherm				Freundlich isotherm			
		q_{max} (mg/g)	B	R_L	R^2	K_f (mg/g)	N	1/n	R^2
Cu	BH	66.67	0.008	0.385-0.926	0.9062	0.9068	1.295	0.772	0.9805
		Temkin isotherm				Dubinin–Radushkevich isotherm			
		A_T(L/mg)	b_T(J/mol)	B	R^2	q_d(mg/g)	B_d(mol^2/kJ^2)	ED(KJ/mol)	R^2
		0.208	264.9	9.3529	0.9214	24.77	2.5*10^{-3}	0.142	0.9171

Adsorption kinetic study

The study of adsorption kinetics in wastewater treatment is important as it not only provides valuable insight into the reaction pathways and the mechanism of sorption reactions, but also describes the solute uptake rate, which in turn control the residence time of sorbate uptake at the solid-solution interface [49-50]. The kinetic data obtained from adsorption of Cu^{2+} ions onto (BH) powder was studied by using four common kinetic models, which are the Pseudo-first order kinetic model, Pseudo-second order kinetic model, Elovich rate equation and Intra-particle diffusion model. The best fit model was selected based on the linear regression correlation coefficient (R^2), which is a measure of how well the predicted values from a forecast model match with the experimental data.

The mechanism adsorption reactions are usually carried out using adsorption reaction models and adsorption diffusion models [51]. Four models are used to understand the kinetics of the reaction.

The pseudo-first-order kinetic model (Lagergren model) assumes that metal ion binds only to one sorption site on the sorbent surface [52]. In Lagergren model, the rate of occupation of biosorption sites is proportional to the number of unoccupied sites [52].

The pseudo first order kinetic rate equation was expressed as:

$$\log(q_e - q_t) = \log(q_e) - \frac{k_1}{2.303}t \qquad \textbf{(Eq. 16)}$$

Where:

q_e and q_t are the amounts of Cu^{2+} ions adsorbed at equilibrium, and at a given time t; k_1 is the rate constant of pseudo first order model.

The pseudo second order is based on the assumption that the rate limiting step may be chemical sorption involving valence forces through sharing or exchange of electrons between heavy metal ions and adsorbent. The pseudosecond order kinetic rate equation was expressed as [49]:

$$\frac{t}{q_t} = \frac{1}{k_2 q_e^2} + \frac{1}{q_e}t \qquad \textbf{(Eq. 17)}$$

Where:

q_e and q_t are the amounts of Cu^{2+} ions adsorbed at equilibrium, and at a given time t;k_2 is the rate constant of pseudo second order.

The applicability of the above two models can be examined by each linear plot of log(q_e-q_t) against t, and (t/q_t) against t, respectively and are represented in Figs (12,13) respectively. The kinetic study for the adsorption of Cu^{2+} ions was performed at optimum pH (7) and completed in 1 h for the concentration 100 mg/L of Cu^{2+} ions onto (0.1, 0.2, 0.3, 0.5 and 0.7 g/200 mL) doses of adsorbent at 25°C.

Fig (12) showed the linear plots of log(q_e-q_t) against t. The k_1 and q_e values were determined from the slope and intercept of the linear plots in Fig (12). Table (3) gave the values of k_1, experimental and calculated values of q_e, as well as the R^2 values for the pseudo-first kinetic plots as can be seen. Although the R^2 values obtained from the plots were low, the theoretical values of q_e were far lower than the corresponding experimental data obtained, these suggesting that the adsorption process did not fit the pseudo-first order kinetic model.

Fig (13) showed the linear plots of (t/q_t) against t. The k_2 and q_e values were determined from the slope and intercept of the linear plots in fig (13) respectively. Table (3) gave experimental calculated values of q_e, as well as the R^2 values for the pseudo- second kinetic plots as can be seen. The theoretical values of q_e were close to the

corresponding experimental data obtained. These suggesting that the adsorption process favorably by the pseudo-second order models.

The Elovich equation has general application to chemisorption kinetics. This equation has been applied satisfactorily to some chemisorption data and has been found to cover a large range of slow adsorption [53]. The Elovich equation is often valid for systems in which the adsorbing surface is heterogeneous. The linearized form is given in equation (18):

$q_t = [1/\beta]\ln[\alpha\beta] + [1/\beta]\ln t$ (Eq. 18)

Where:

α(mg/g.min) is the initial adsorption rate and β (g/mg) is the de-sorption constant during any experiment. The Elovich constants are determined from the linear plot of q_t versus ln(t)as presented in fig (14) and table (4) for Cu(II) ions. The regression R^2 value is ranged between 0.9526 and 0.9302 for Cu^{2+}ions. This indicate that applicapility of this model to the experimental data obtained for the adsorption of Cu(II) onto (BH).

Weber-Morris mechanistic model in equation (19), [54] was used to ascertain whether intra-particle diffusion or film diffusion (external diffusion) is the rate-controlling step.

$q_t = k_{dif}\, t^{1/2} + I$ (Eq. 19)

Where:

k_{dif} is the intra-particle diffusion rate constant (mg/g.$min^{0.5}$) and I (mg/g) is constant describing the thickness of the boundary layer. A linear plot of q_t versus $t^{0.5}$ passing through the origin will suggest intra-particle diffusion as the sole rate determining step [55-61]. However, if a linear plot was obtained that is not passing through the origin, it means the adsorption process is controlled by more than one mechanism. In this study, a linear plot was obtained that did not pass through the origin fig (15), suggesting that the mechanism of the reaction is multi-linear and the rate-limiting reaction is controlled both through film diffusion and intra-particle diffusion.

Values of (I) in equation (19) varied from 27.034 to 15.725 mg/g for Cu^{2+}. The value of (I) decreased with increasing the adsorbent dose this decreasing reflect that decrease of thickness of boundary layer and the chance of external mass transfer to increase is high.

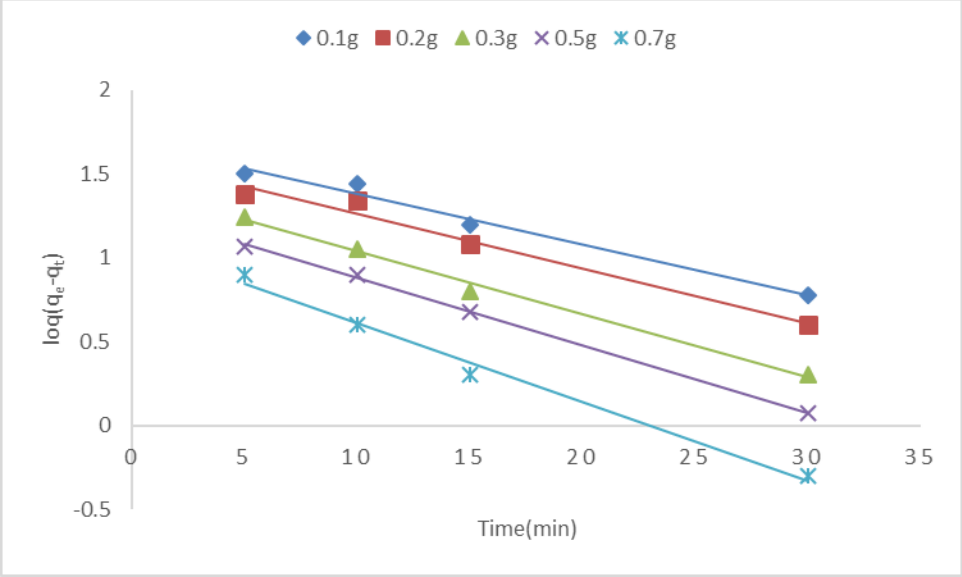

Figure 12: Pseudo-first order kinetic fit for adsorption of Cu(II) onto BH at different adsorbent dose, the initial concentration=100ppm, 400 rpm and 298^oK.

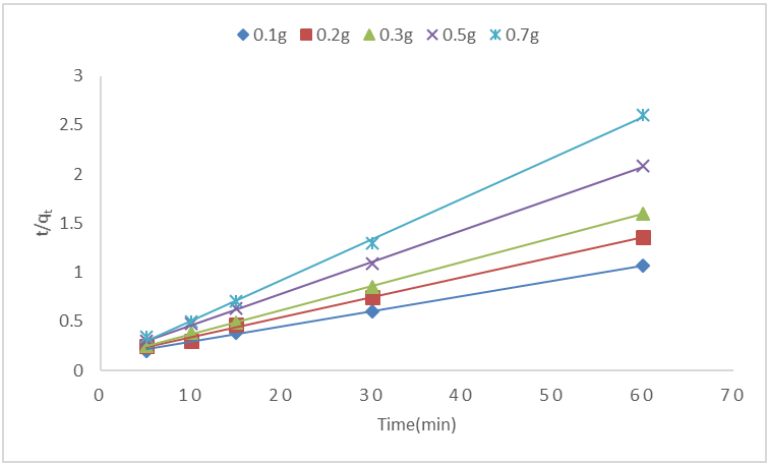

Figure 13: Pseudo- second order kinetic fit for adsorption of Cu(II)onto BH at different adsorbent, initial concentration=100ppm, 400 rpm and 298°K.

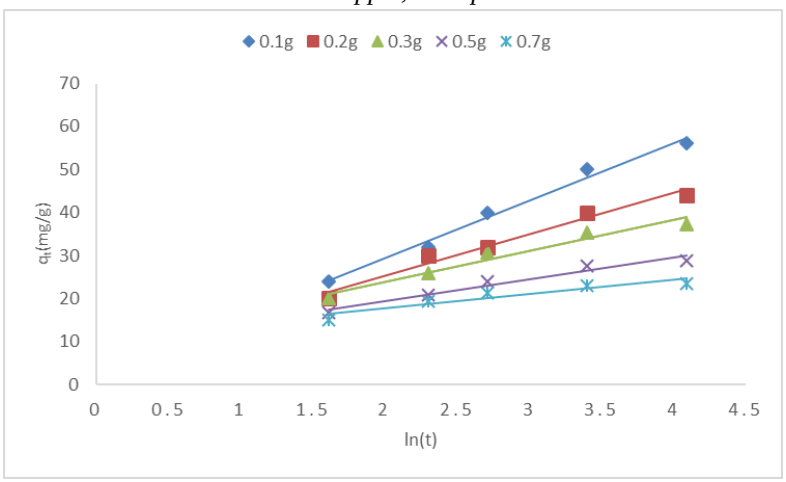

Figure 14: Elovich model plot for adsorption of Cu(II) onto BH at different adsorbent dose, initial concentration=100ppm, 400 rpm and 298°K.

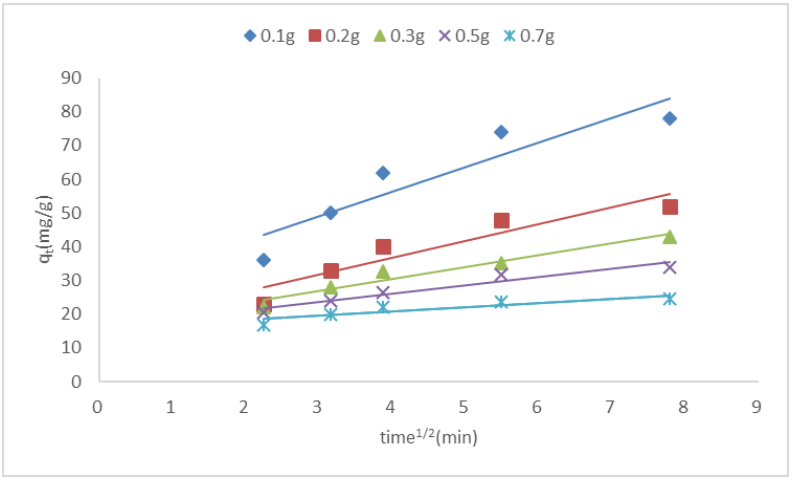

Figure 15: Intra particle diffusion model plot for adsorption of Cu(II) onto BH at different adsorbent dose, initial concentration=100ppm, 400 rpm and 298°K.

Table 3: Kinetic models Pseudo-first order, Pseudo-second order equations and other parameters for adsorption of Cu(II) onto BH at different adsorbent dose of metal ions, initial concentration=100ppm, 400 rpm and 298^{o}K**.**

Dose of adsorbent (g)	Pseudo first-order				Pseudo second-order			
	k_1 (min^{-1})	q_e (mg/g)		R^2	k_2 (g/mg.min)	q_e (mg/g)		R^2
		exp	calc			exp	calc	
0.1g	0.061	124	69.75	0.9350	0.00150	124	135.14	0.9985
0.2g	0.082	70	48.49	0.9921	0.00345	70	74.07	0.9977
0.3g	0.062	52	24.10	0.9640	0.00663	52	52.63	0.9995
0.5g	0.043	32	6.74	0.9286	0.01998	32	32.26	0.9996
0.7g	0.068	25.4	6.11	0.9610	0.03211	25.4	25.58	0.9998

Table 4: Kinetic models Elovich model, Intra particle diffusion model and other parameters for adsorption of Cu(II) onto (BH) at different adsorbent dose of metal ions, initial concentration=100ppm,400 rpm and 298^{o}K

Kinetic models	Parameters	Dose of adsorbent				
		0.1(g)	**0.2(g)**	**0.3(g)**	**0.5(g)**	**0.7(g)**
Elovich model						
	β (g/mg)	0.0568	0.0838	0.1130	0.1745	0.3219
	α (mg/g.min)	0.916	0.914	0.421	0.216	0.017
	R^2	0.9526	0.9693	0.9809	0.9877	0.9302
Intra particle diffusion model						
	k_{dif} (mg/g.$min^{0.5}$)	7.3159	4.9963	3.5137	2.4627	1.2771
	I(mg/g)	27.034	16.686	16.367	16.163	15.725
	R^2	0.8433	0.8747	0.9461	0.9387	0.8089

Conclusion

This work examined the adsorption of metal (Cu^{2+}) from aqueous solution using bean husk powder. Through this experimental study, it has been shown that the bean husk can be used as low cost adsorbent material for the removal of Cu^{2+}ions from aqueous solution. Various parameters such as contacting time, pH of solution, initial concentration, temperature, and adsorbent dose have been investigated. The isotherm study for copper adsorption onto bean husk has shown that, the Freundlich isotherm model was the best. The kinetic study has shown that the adsorption process of the Pseudo-first order, Pseudo- second order, Elovich equation and Intra-particle diffusion model and the rate constants of them have been determined. The thermodynamic study has shown that the adsorption process is spontaneous, since the calculated Gibbs free energy values were decreased with increasing the temperature and endothermic process, since the enthalpy was positive value.

References

[1]. Wattoo. M.H.S., Iqbal J., Kazi .T.G and Jakhrani. M.A., "Monitoring of pollution parameters in waste of tanneries in Kasur ", Pak J, Biolog, Sci, 2000.

[2]. Wattoo. M.H.S., Wattoo. F.H., Tirmizi S.A., Kazi T.G., Bhanger M.I. and Ibex J "Pollution of Phulali canal water in the city premises of Hyderabad: Metal monitoring". J. Chem, Soc, Pak, 2006.

[3]. Sari. A., Tuzen. M., C1tak. D. and Soylak. M., "Adsorption characteristics of Cu(II) and Pb(II) onto expanded perlite from aqueous solution" J Hazardous Mater, 2007.

[4]. Tewari. N., Vasudervan P. and Guha B.K., "Study on biosorption of Cr(III) by Mucorhiemalis" Bioche, Eng J, 2005.

[5]. Kýlýç M, Kýrbýyýk Ç, Çepelioðullar Ö, Pütün AE. Adsorption of heavy metal ions from aqueous solutions by bio-char, a by-product of pyrolysis. Appl Surf Sci, 2013.

[6]. Meena AK, Kadirvelu K, Mishraa GK, Rajagopal C, Nagar PN. Adsorption of Pb(II) and Cd(II) metal ions from aqueous solutions by mustard husk. J Hazard Mater, 2008.
[7]. Ahmed, A.M., Ali, A.E., Ghazy, A.M. Adsorption Separation of Nickel from Wastewater by using Olive Stones. Advanced Journal of Chemistry-Section A, 2019.
[8]. Sarý A, Uluozlü ÖD, Tüzen M. Equilibrium, thermodynamic and kinetic investigations on biosorption of arsenic from aqueous solution by algae (Maugeotiagenu flexa) biomass. Chem Eng J, 2011.
[9]. Wu, D.B., Nia, C, J., Li, D.Q. and Bai, Y. Solvent extraction of scandium (III), yttrium (III), lanthanum III) and gadolinium (III) using Cyanic (III) and gadolinium (III) using Cyanic (302 in heptane. J of Alloys and Compounds, 2004.
[10]. Babel, S. and Kurniawan, T.A. Various treatment technologies to remove arsenic and mercury from contaminated groundwater: an overview. In: Proceedings of the First International Symposium on Southeast Asian Water Environment, Bangkok, Thailand, 24-25 October, 2003.
[11]. Process of Heavy Metals by Low-Cost Adsorbent: A Review. World Applied Sci, J 2013.
[12]. Masoud, M.S., El-Saraf, W.M., Abdel – Halim, A.M., Ali, A.E., Mohamed, E.A., Hasan, H.M.I. Rice husk and activated carbon for waste water treatment of El-Mex Bay, Alexandria Coast, Egypt. Arabian Journal of Chemistry, 2016.
[13]. Giles C.H., Macewan T.H., Nakhwa S.N. and Smith D.," A system of classification of solution adsorption isotherms, and its Use in Diagnosis of adsorption mechanisms and in measurement of specific surface areas of solids". J, Chem, Soc, 1960.
[14]. Patra J.M. Biochar as a low –cost adsorbent for heavy metal removal. Biosciences, 2017. Ghaedi M, Hajati S, Karimi F, Barazesh B, Ghezelbash G. Equilibrium, kinetic and isotherm of some metal ion biosorption. J Ind, Eng Chem, 2013.
[15]. Aichour, A., Zaghouane-Boudiaf, H., Iborra, C.V., Polo, M.S. Bioadsorbent beads prepared from activated biomass/alginate for enhanced removal of cationic dye from water medium: kinetics, equilibrium and thermodynamic studies. J Mol, Liq, 2018.
[16]. Feng N, Guo X, Liang S, Zhu Y, Liu J. Biosorption of heavy metals from aqueous solutions by chemically modified orange peel. J Hazard Mater, 2011.
[17]. Farooq U, Kozinski J a, Khan MA, Athar M. Biosorption of heavy metal ions using wheat based biosorbents--a review of the recent literature. Bioresour Technol, 2010.
[18]. Gupta VK, Rastogi A, Nayak A. Biosorption of nickel onto treated alga (Oedogoniumhatei): Application of isotherm and kinetic models. J Colloid Interface, Sci, 2010.
[19]. Naiya TK, Bhattacharya AK, Mandal S, Das SK. The sorption of lead(II) ions on rice husk ash. J Hazard Mater, 2009.
[20]. Gregorio, C., Harmel, N.P., Frederic, G., Capucine, R. Removal of C.I. basic Green 4 (Malachite Green) from aqueous solutions by adsorption using cyclodextrin-based adsorbent: kinetic and equilibrium studies. Sep, Purif. Technol, 2007.
[21]. Onal, Y. Kinetics of adsorption of dyes from aqueous solution using activated carbon prepared from waste apricot. J Hazard Mater B, 2006.
[22]. Weber, W.J., DiGiano, F.A. Process dynamics in environmental systems. John Wiley & Sons, Inc. New York, 1996.
[23]. Abdel-Ghani N, Hefny M, El-Chaghaby G. Removal of lead from aqueous solution using low cost abundantly available adsorbents, 2007.
[24]. Yang S., Li J., Shao D., Hu J., Wang X. Adsorption of Ni (II) on oxidized multi-walled carbon nanotubes: effect of contact time, pH, foreign ions and PAA. J of Hazardous Materials, 2009.
[25]. Kumar D, Gaur JP. Metal biosorption by two cyanobacterial mats in relation to pH, biomass concentration, pretreatment and reuse. Bioresour Technol, 2011.

[26]. Rao, M.M., Rao, G.P.C., Seshaiah, K., Choudary, N.V., Wang, M.C. Activated carbon from Ceibapentandra hulls, an agricultural waste, as an adsorbent in the removal of lead and zinc from aqueous solutions. Waste Manage, 2008.
[27]. Silva, C., Gama, B., Gonçalves, A., Medeiros, J., & Abud, A. Basic-dye adsorption in albedo residue: effect of pH, contact time, temperature, dye concentration, biomass dosage, rotation and ionic strength. J King Saud, Univ. Eng, Sci, 2019.
[28]. Seow, W. T. & Lim, K. C. Removal of dye by adsorption: a review. Int J Appl, Eng, Res, 2016.
[29]. Albroomi, I. H., Elsayed, A., Baraka, A. & Abdelmaged, A. Batch and fixed-bed adsorption of tartrazine azo-dye onto activated carbon prepared from apricot stones. Appl, Water Sci, 2017.
[30]. Choi, H. Agricultural bio-waste for adsorptive removal of crude oil in aqueous solution. J of Material Cycles and Waste Management, 2019.
[31]. Younes, S.M., Elabdeen, A.Z, Ali, A.E., Salem, W.M. Ferrite Nanocomposite (Rice Straw- CoFe2O4) as New Chemical Modified for Treatment of Heavy Metal from Waste Water. Journal of Hydrology: Current Research, 2019.
[32]. Broznic D., Milin C. Effects of temperature on sorption desorption processes of imidacloprid in soils of Croatian coastal regions. J of Environ, Sci and Health B, 2012.
[33]. Zaki, A.B., El-Sheikh, M.Y., Evans, J. and El-Safty, S.A. Kinetics and mechanism of the sorption of some aromatic amines onto amberlite IRA-904 anion-exchange resin. J Colloid, Interf, Sci, 2000.
[34]. Gupta, V.K. Equilibrium uptake, sorption dynamics, process development, and column operations for the removal of copper and nickel from aqueous solution and wastewater using activated slag, a low-cost adsorbent. Ind, Eng, Chem, Res, 1998.
[35]. Hameed, B.H.; Chin, L.H.; Rengaraj, S. Adsorption of 4-chlorophenol onto activated carbon prepared from rattan sawdust. Desalination, 2008.
[36]. Rehman, M.S.; Kim, I.; Han, J.I. Adsorption of methylene blue dye from aqueous solution by sugar extracted spent rice biomass. Carbohydr, Polym, 2012.
[37]. Farhan AM, Al-Dujaili AH, Awwad AM. Equilibrium and kinetic studies of cadmium(II) and lead(II) ions biosorption onto Ficuscarcia leaves. Int J IndChem, 2013.
[38]. Moyo, M.; Chikazaza, L. Bioremediation of lead(II) from polluted wastewaters employing sulphuric acid treated maize tassel biomass. Am J Anal, Chem, 2013.
[39]. Gupta, V.K.; Shrivastava, A.K.; Jain, N. Biosorption of chromium (VI) from aqueous solutions by green algae spirogyra species. Water Res, 2001.
[40]. Freudlich, H.T.M. Over the adsorption in solution. J of physical chem, 1906.
[41]. Olorundare, O.F.; Msagati, T.A.M.; Krause, R.W.M.; Okonkwo, J.O.; Mamba, B.B. Steam activation, characterization and adsorption studies of activated carbon from maize tassels. ChemEcol, 2014.
[42]. Schulthess C. P., Sparks D. L. Advances in Soil Science. Berlin, Germany: Springer. Equilibrium-based modeling of chemical sorption on soils and soil constituents, 1991.
[43]. Dada, A.O., Olalekan, A.P., Olatunya, A.M., Dada, O. Langmuir, Freundlich, Temkin and Dubinin–Radushkevich Isotherms Studies of Equilibrium Sorption of Zn2+ Unto Phosphoric Acid Modified Rice Husk. IOSR. J of Applied Chem, (IOSR-JAC), 2012.
[44]. Boparai HK, Joseph M, O. Carroll DM. Kinetics and thermodynamics of cadmium ion removal by adsorption onto nano zero valent iron particles. J Hazard Mater, 2011.
[45]. Hutson ND, Yang RT., Theoretical basis for the Dubinin Radushkevitch (D.R) adsorption isotherm equation. Adsorption, 1997.
[46]. Horsfall M, Spiff AI, Abia AA. Studies on the influence of mercapto acetic acid (MAA) modification of cassava (manihotsculentacranz) waste biomass on the adsorption of Cu^{+2} and Cd^{2+} from aqueous solution. Korean Chem, Soc, 2004.

[47]. Itodo AU, Happiness UO, Obaroh IO, Usman A, Audu SS. Temkin, RD, Langmuir and Freundlich adsorption Isotherms of industrial dye uptake unto H_3PO_4 catalyzed poultry waste bioadsorbent. J of Sci, Technol research, 2009b.
[48]. Monika J, Garg V, Kadirvelu K. Chromium (VI) removal from aqueous solution, using sunflower stem waste. J Hazardous materials, 2009.
[49]. Ho, Y.S. and McKay, Pseudo-second order model for sorption processes. Process Biochemi, 1998.
[50]. Masoud, E.S., Ali, A.E., Hassan, A.F., Hassan, H.S., Elkady, M.F. Kinetics, Equilibrium and Thermodynamic Behavior of Potential Removal of Reactive Dye onto Zinc Oxide Nanotubes. Journal of Bulletin of Faculty of Science, 2014.
[51]. Ahmad, R.; Kumar, R.; Laskar, M.A. Adsorptive removal of Pb^{+2} form aqueous solution by macrocyclic calyx [4] naphthalene: Kinetic, thermodynamic, and isotherm analysis. Environ, Sci, Pollut, Res, 2013.
[52]. Ghaedi M, Hajati S, Karimi F, Barazesh B, Ghezelbash G. Equilibrium , kinetic and isotherm of some metal ion biosorption. J Ind Eng Chem, 2013.
[53]. Low MJD, Kinetics of chemisorption of gases on solids. Chem Reviews, 1960.
[54]. Weber, W.J.; Morris, J.C. Kinetics of adsorption on carbon from solution. J Sanit. Eng, Div, 1963.
[55]. Olu-Owolabi, B.I.; Diagboya, P.N.; Adebowal, K.O. Evaluation of pyrene sorption desorption on tropical soils. J Environ. Manag, 2014.
[56]. Masoud M.S., Ali A.E., Elasala G.S., Kolkaila S.A. Spectroscopic studies and thermal analysis on cefoperazone metal complexes, J. Chem. Pharm, 2017.
[57]. Ali A. E., Elasala G. S., Mohamed E. A. Kolkaila, S.A., J. materials today proceeding https://doi.org/10.1016/j.matpr.2020, 2021.
[58]. Ali A. E., Elasala G. S., Mohamed E. A., Kolkaila S.A., Spectral, thermal studies and biological activity of pyrazinamide complexes, heliyon, 2019.
[59]. Masoud M.S., Ali A.E., Elasala G.S., Sakr S.F, kolkailas. A., Structural, J. Chem. Pharm, 2020.
[60]. Ali A.E., Elasala G.S., Ibrahim S. Ibrahim., Kolkailas. A. Synthesis, characterization, spectral, thermal analysis and biological activity studies of some montelukast sodium complexes, J. Chemical Research Advances, 2021.
[61]. Shaban N.Z., Ali A.E., Masoud M.S., J. Inorg. Biochem, 2003.